Electronic Supplementary Material (ESI) for Physical Chemistry Chemical Physics.

Solid-Ionic Liquid-Interfaces: Pore Filling Revisited

M. T. Heinze*, J. C. Zill, J. Matysik, W.D. Einicke, R. Gläser, A. Stark*

Supplementary Information

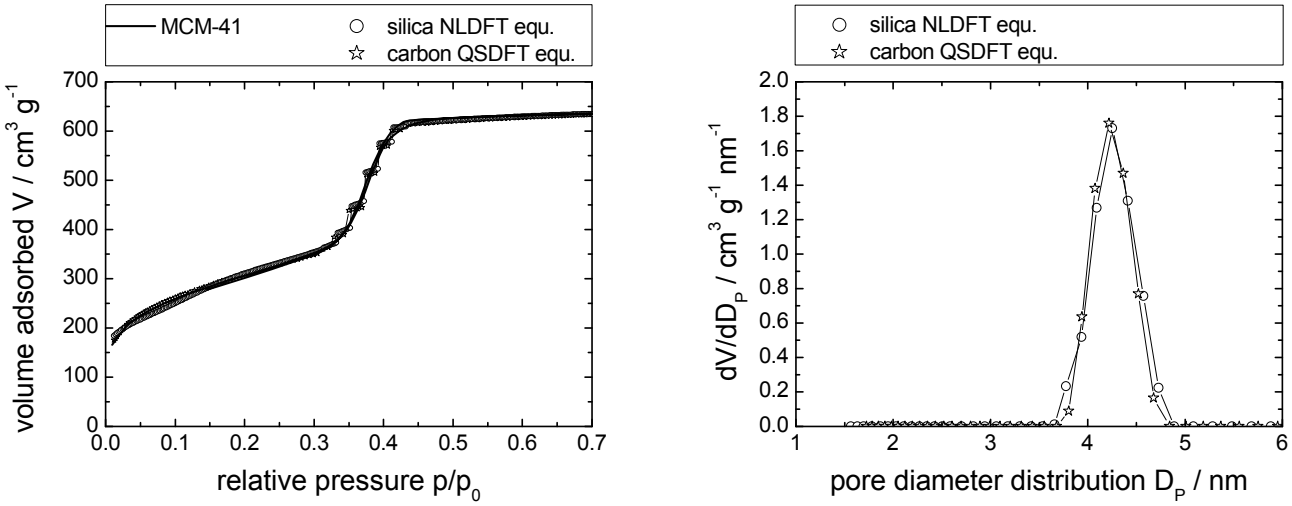

Figure SI 1a: N_2-sorption isotherm of the pristine MCM-41 (left; measured: squares; calculated using NLDFT and QSDFT: open circles and open stars, respectively), and resulting pore diameter distributions (right).

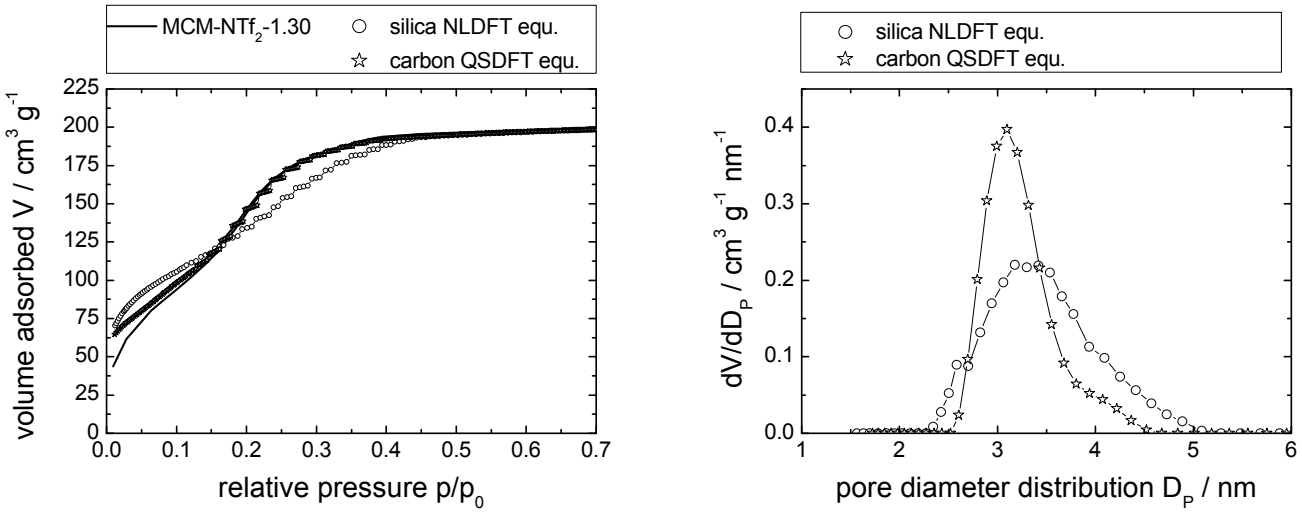

Figure SI 1b: N_2-sorption isotherm of MCM-NTf_2-1.30 (left; measured: squares; calculated using NLDFT and QSDFT: open circles and open stars, respectively), and resulting pore diameter distributions (right).

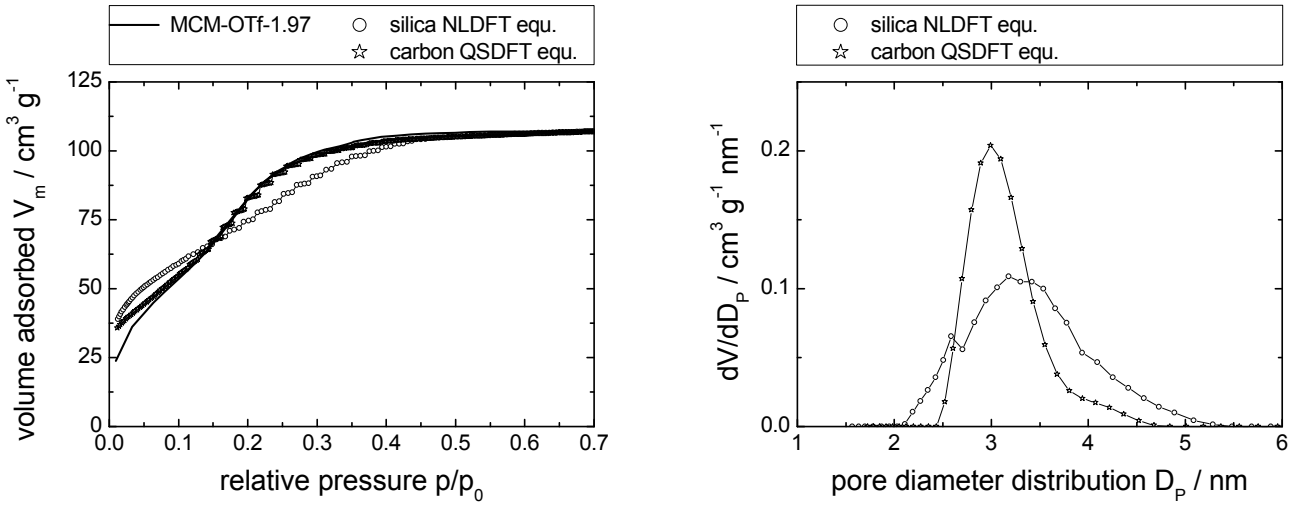

Figure SI 1c: N_2-sorption isotherm of MCM-OTf-1.97 (left; measured: squares; calculated using NLDFT and QSDFT: open circles and open stars, respectively), and resulting pore diameter distributions (right).

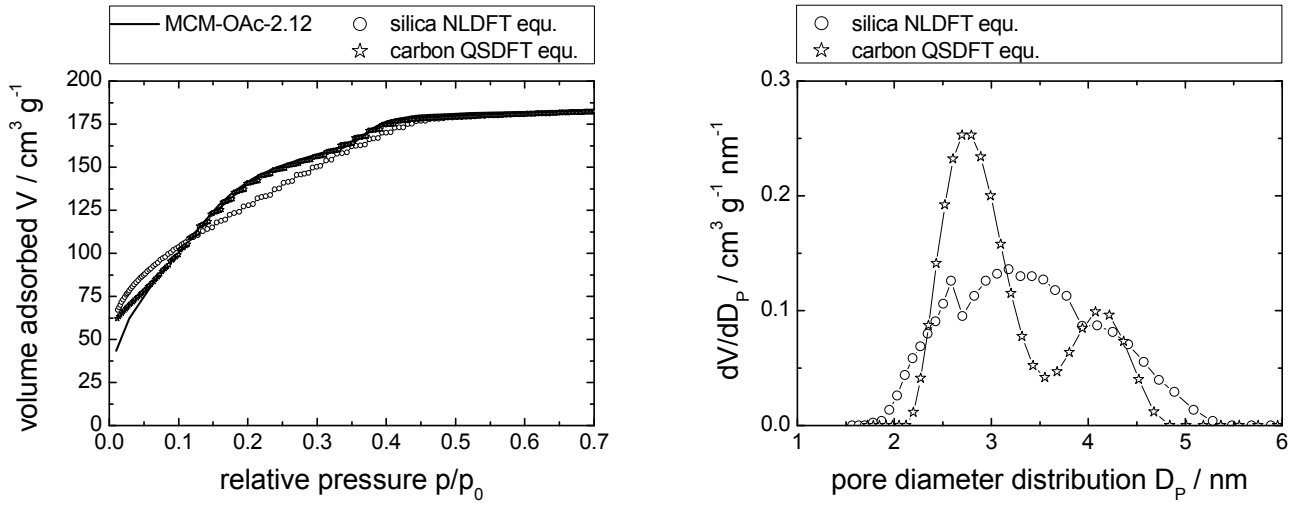

Figure SI 1d: N_2-sorption isotherm of MCM-OAc-2.12 (left; measured: squares; calculated using NLDFT and QSDFT: open circles and open stars, respectively), and resulting pore diameter distributions (right).

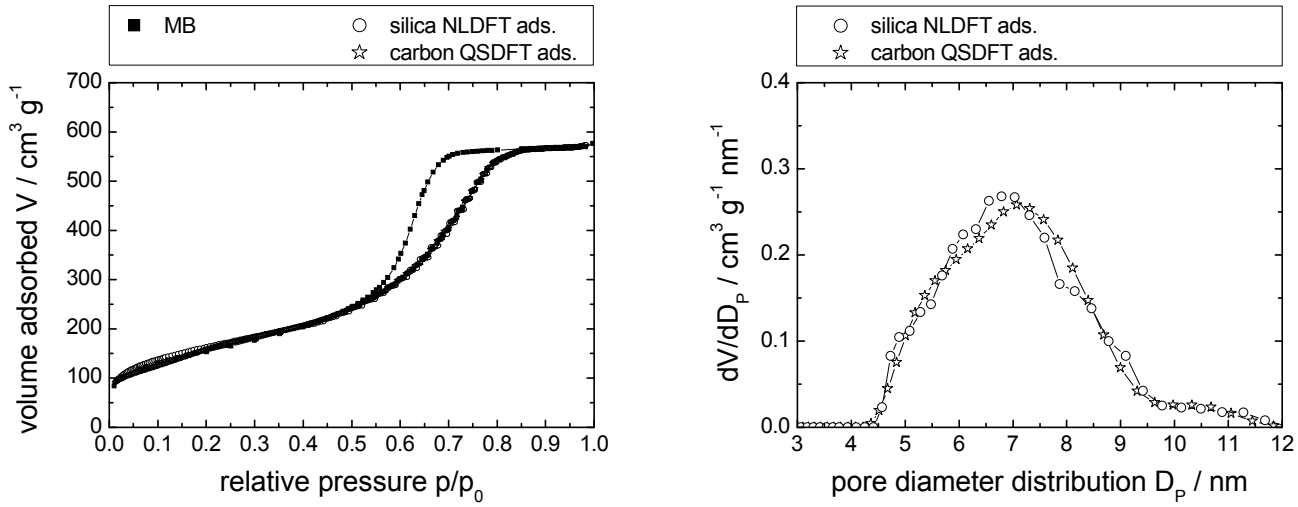

Figure SI 2a: N_2-sorption isotherm of pristine MB (left; measured: squares; calculated using NLDFT and QSDFT: open circles and open stars, respectively), and resulting pore diameter distributions (right).

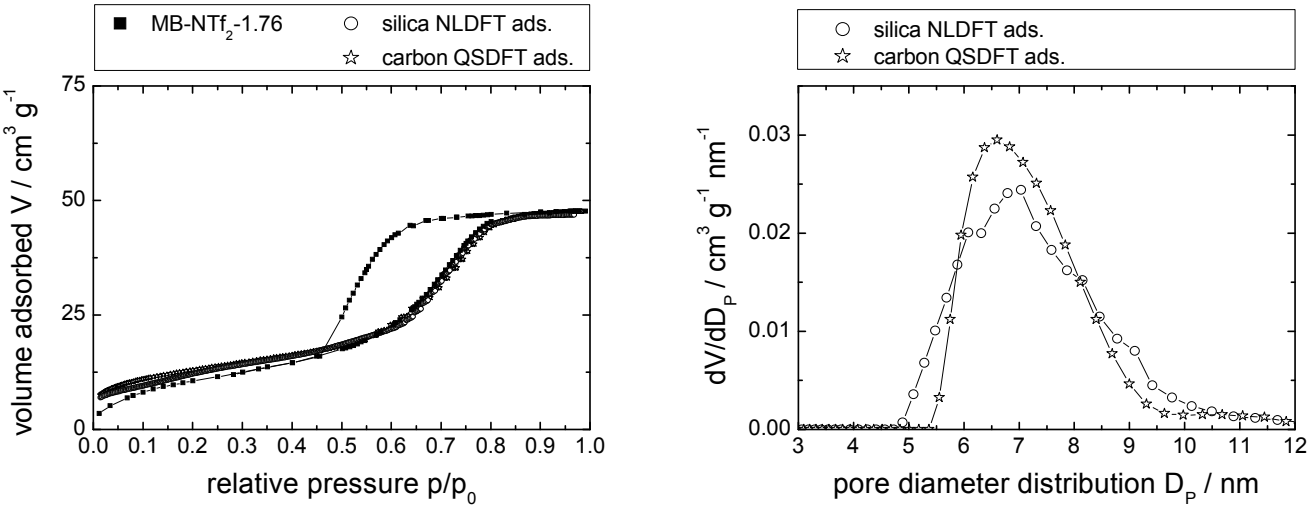

Figure SI 2b: N_2-sorption isotherm of MB-NTf_2-1.76 (left; measured: squares; calculated using NLDFT and QSDFT: open circles and open stars, respectively), and resulting pore diameter distributions (right).

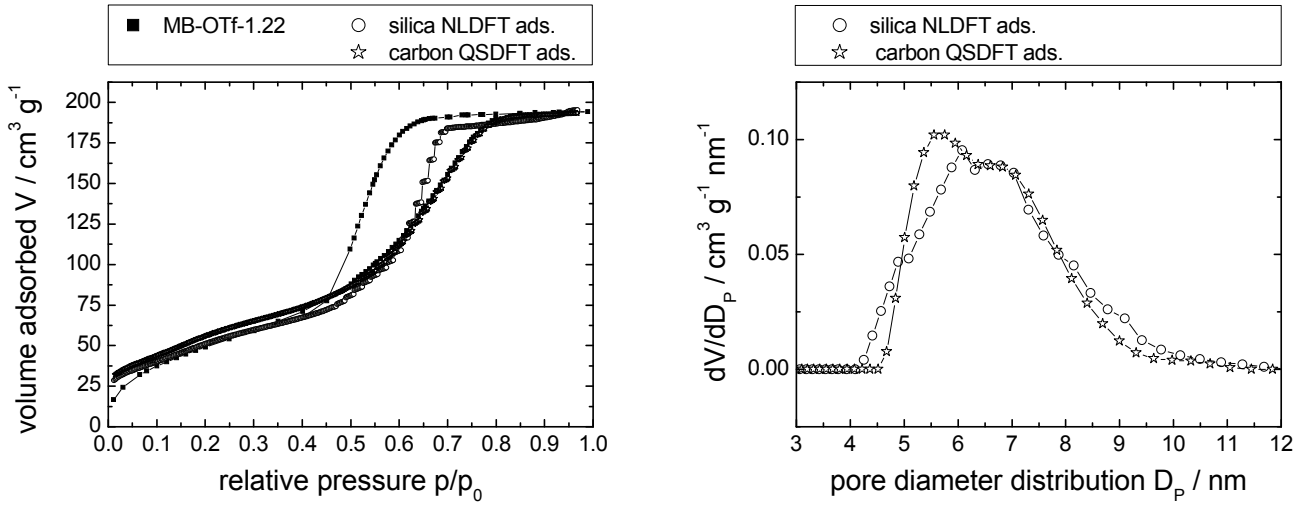

Figure SI 2c: N_2-sorption isotherm of MB-OTf-1.22 (left; measured: squares; calculated using NLDFT and QSDFT: open circles and open stars, respectively), and resulting pore diameter distributions (right).

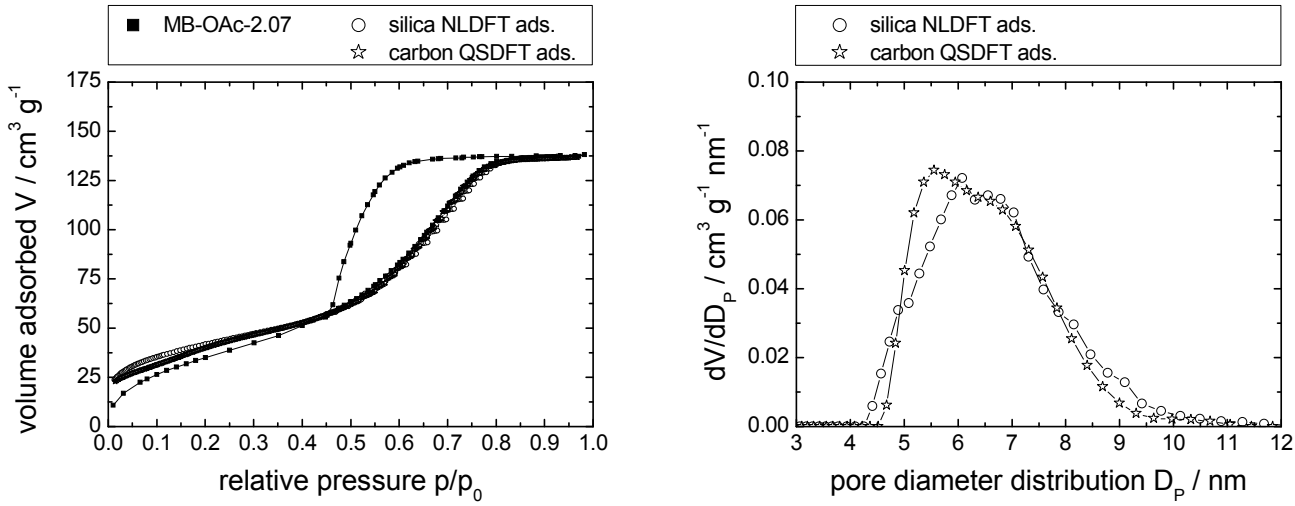

Figure SI 2d: N_2-sorption isotherm of MB-OAc-2.07 (left; measured: squares; calculated using NLDFT and QSDFT: open circles and open stars, respectively), and resulting pore diameter distributions (right).

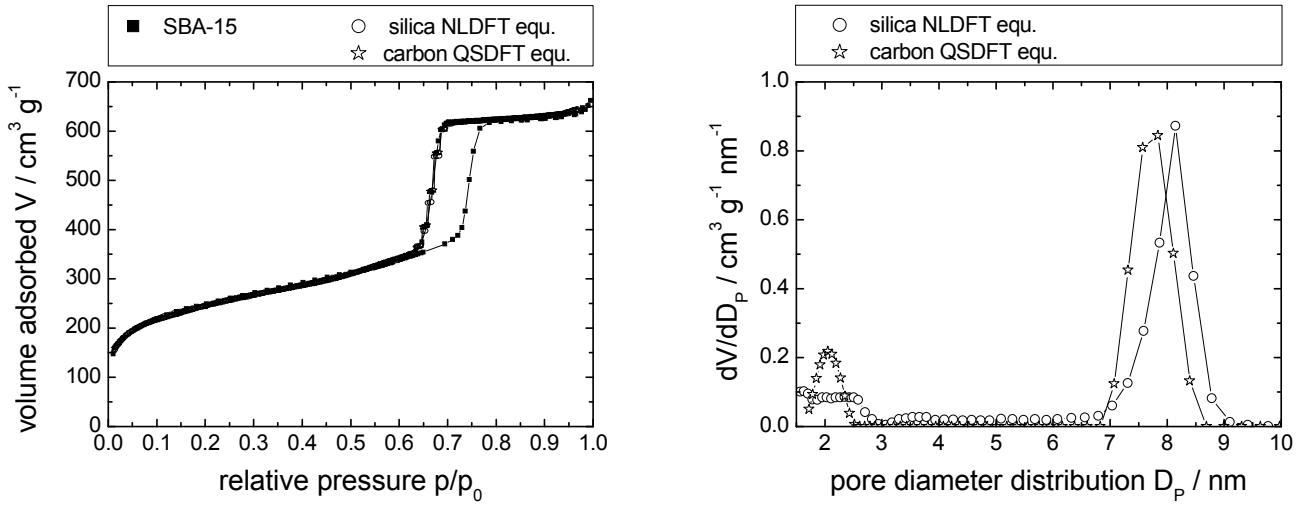

Figure SI 3a: N_2-sorption isotherm of pristine SBA-15 (left; measured: squares; calculated using NLDFT and QSDFT: open circles and open stars, respectively), and resulting pore diameter distributions (right).

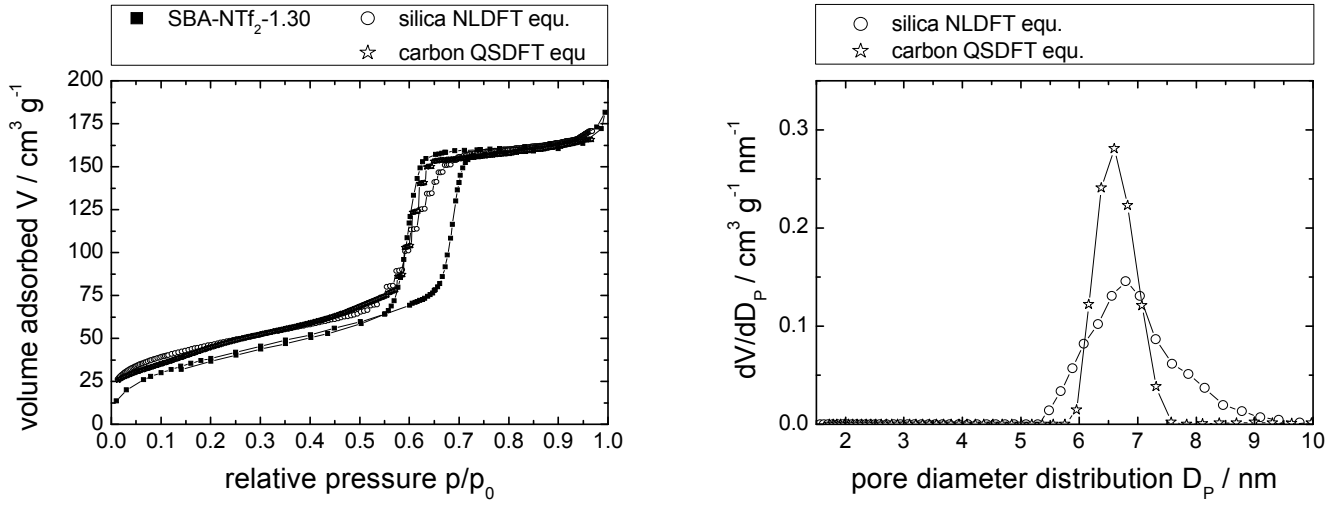

Figure SI 3b: N_2-sorption isotherm of SBA-NTf_2-1.30 (left; measured: squares; calculated using NLDFT and QSDFT: open circles and open stars, respectively), and resulting pore diameter distributions (right).

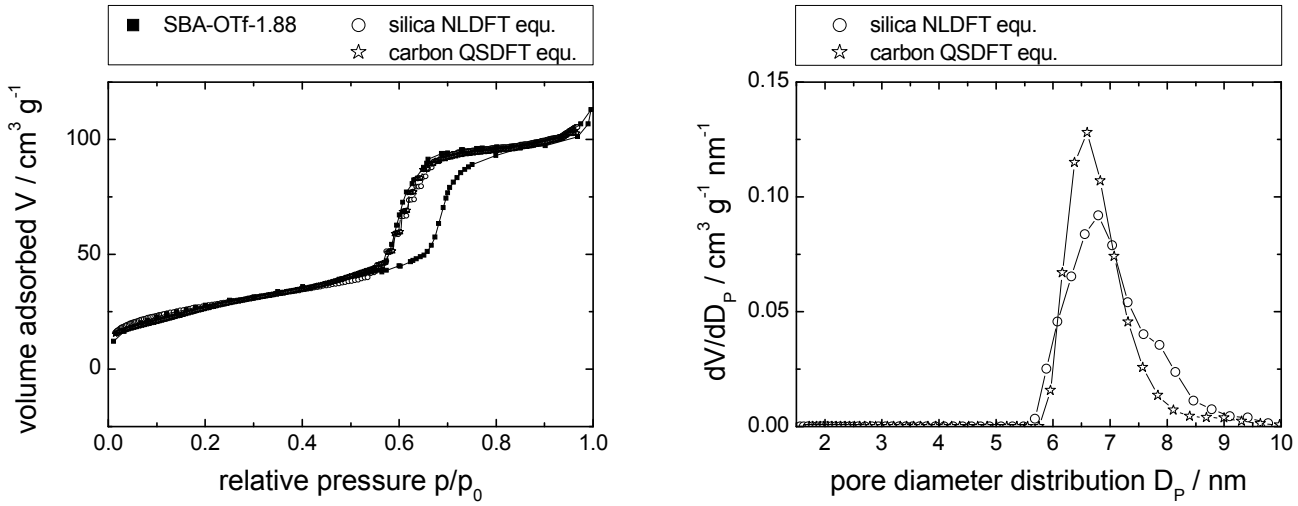

Figure SI 3c: N_2-sorption isotherm of SBA-OTf-1.88 (left; measured: squares; calculated using NLDFT and QSDFT: open circles and open stars, respectively), and resulting pore diameter distributions (right).

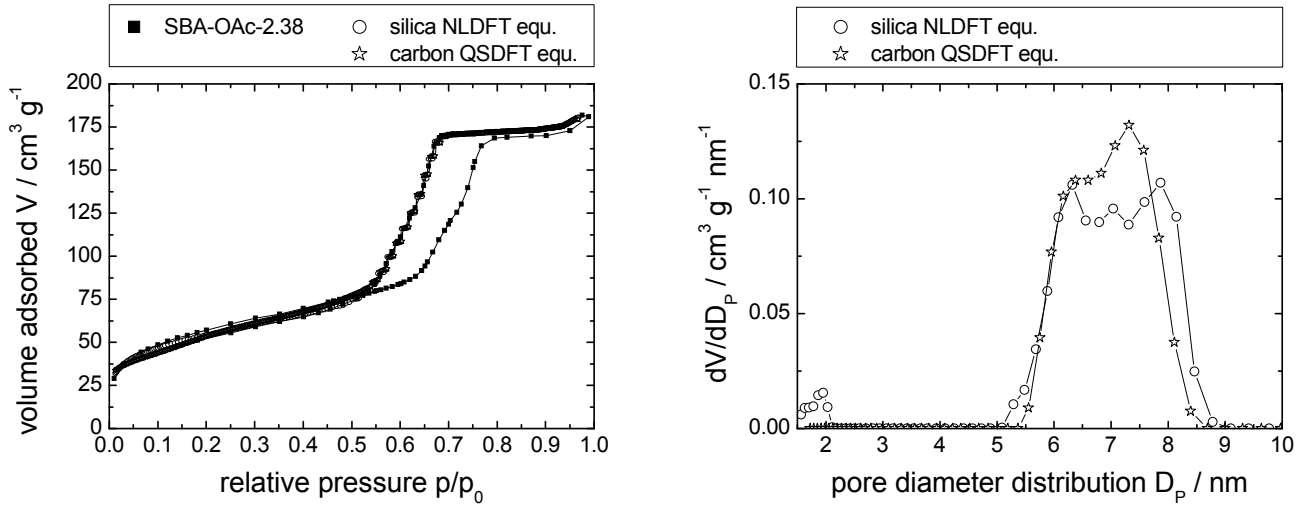

Figure SI 3d: N_2-sorption isotherm of SBA-OAc-2.38 (left; measured: squares; calculated using NLDFT and QSDFT: open circles and open stars, respectively), and resulting pore diameter distributions (right).

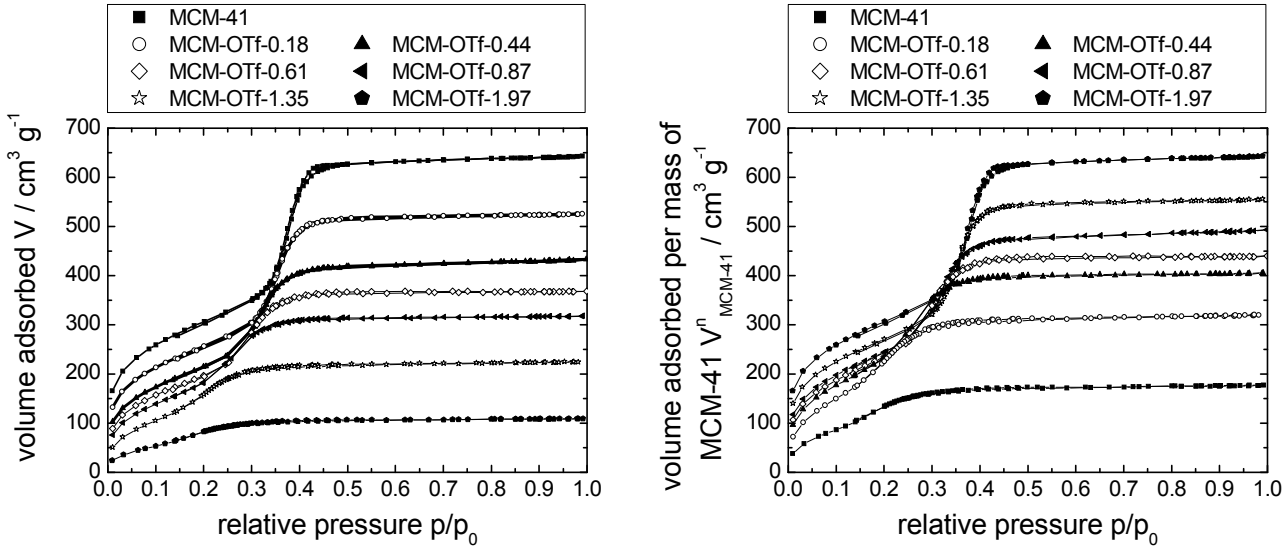

Figure SI 4: N_2-sorption isotherms at 77 K of MCM-41-based materials impregnated with incrementally increasing amounts of [C_6mim][OTf], as volume absorbed per mass of material (left) and as volume absorbed per mass of support (right).

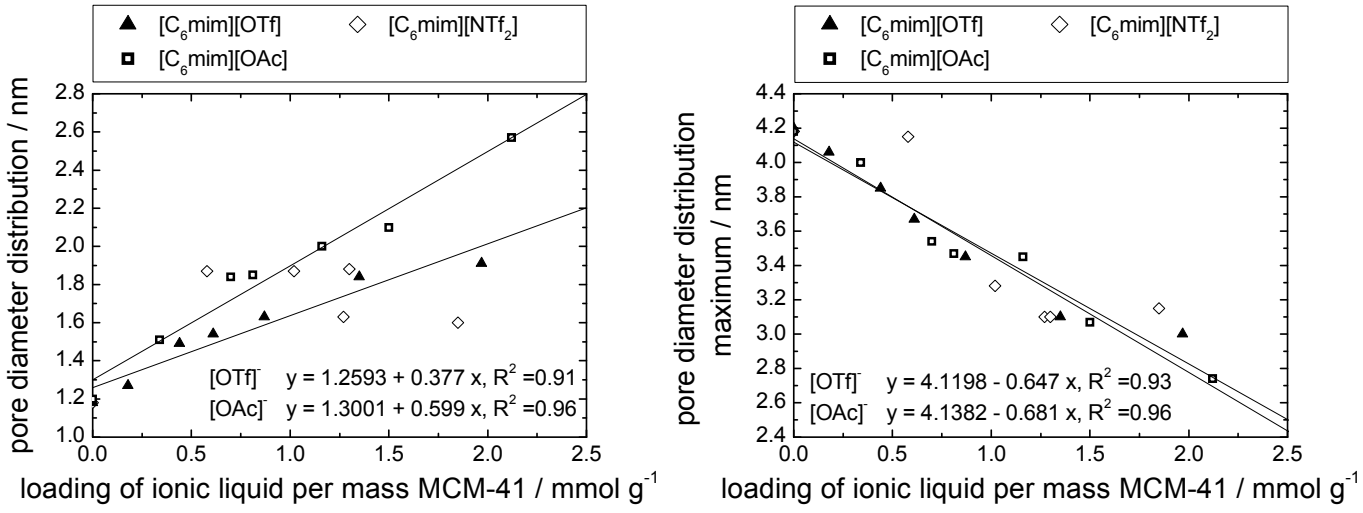

Figure SI 5: Pore diameter distribution vs. loading, and pore diameter distribution maximum vs. loading for all ionic liquids investigated on MCM-41.

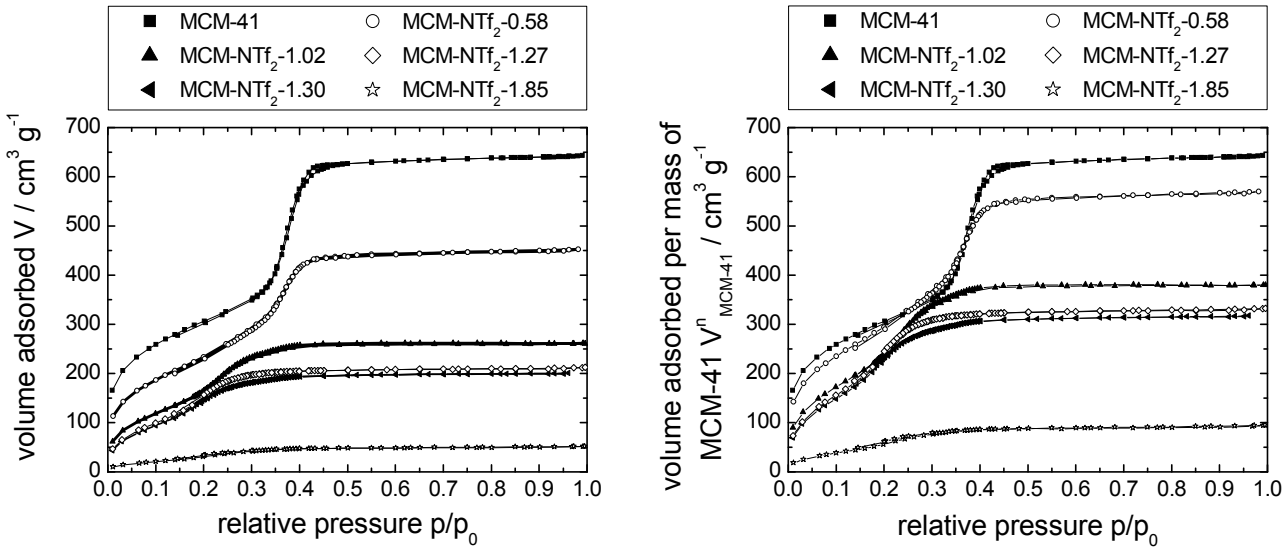

Figure SI 6: N_2-sorption isotherms at 77 K of MCM-41-based materials impregnated with incrementally increasing amounts of $[C_6mim][NTf_2]$, as volume absorbed per mass of material (left) and as volume absorbed per mass of support (right).

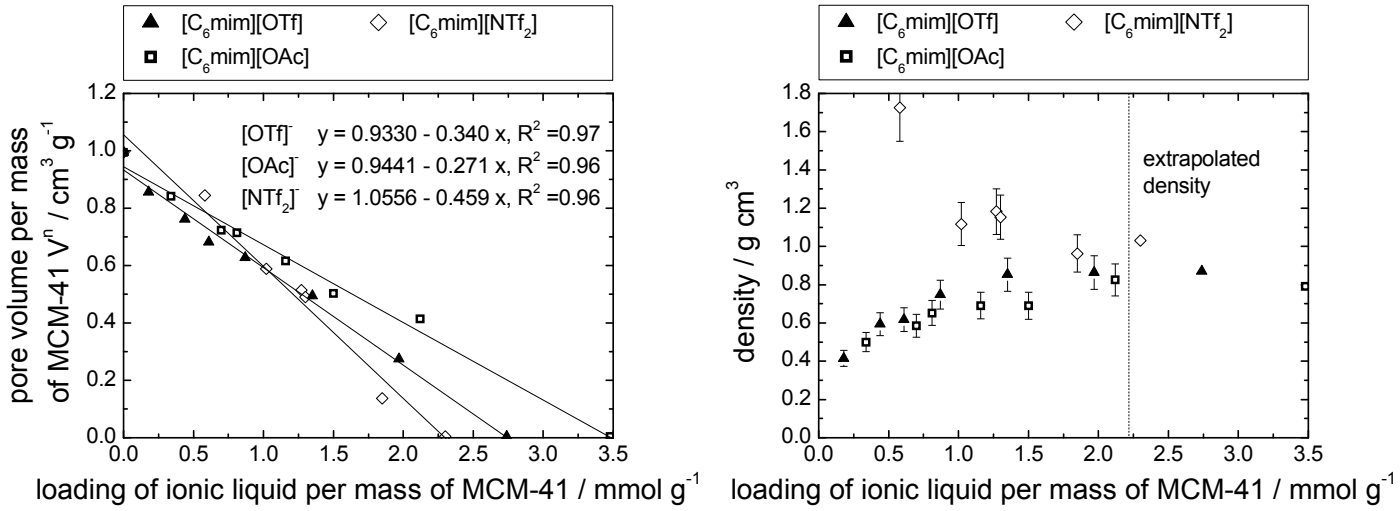

Figure SI 7: Pore volume vs. loading, and density vs. loading of MCM-41 modified with incrementally increasing amounts of the ionic liquids investigated. The theoretical loading for complete pore filling ($V_n = 0$) is linearly extrapolated from the experimental data.

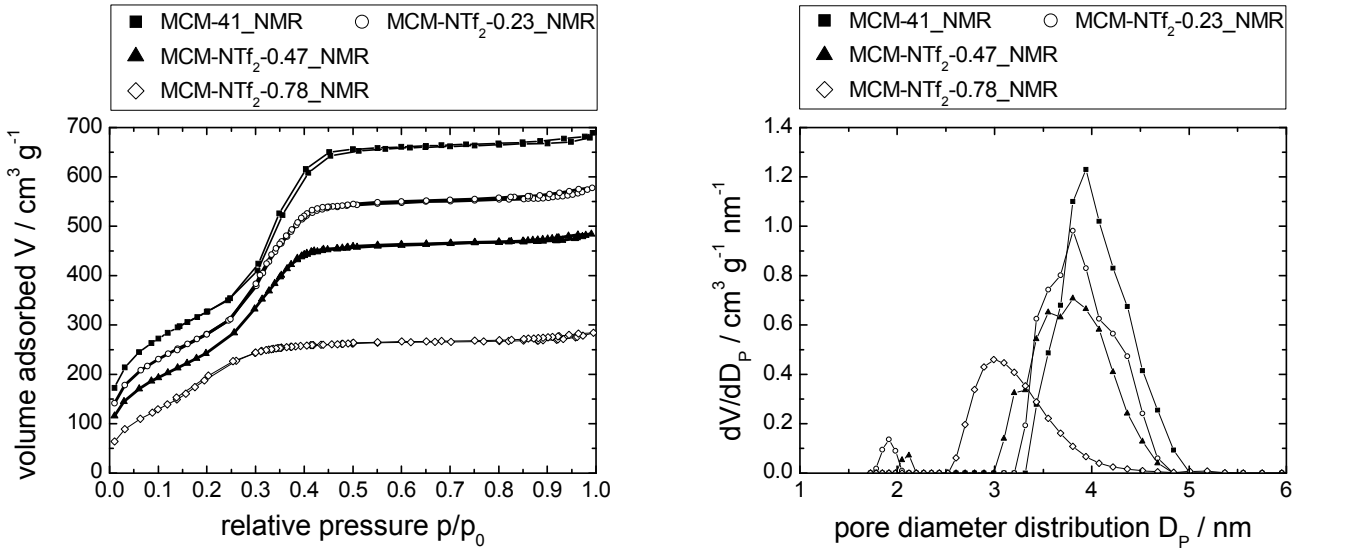

Figure SI 8: N_2-sorption isotherms at 77 K of MCM-41_NMR, and of MCM-41_NMR modified with $[C_6mim][NTf_2]$ (left) and pore diameter distribution (right) of MCM-41_NMR, and of MCM-41_NMR modified with $[C_6mim][NTf_2]$.

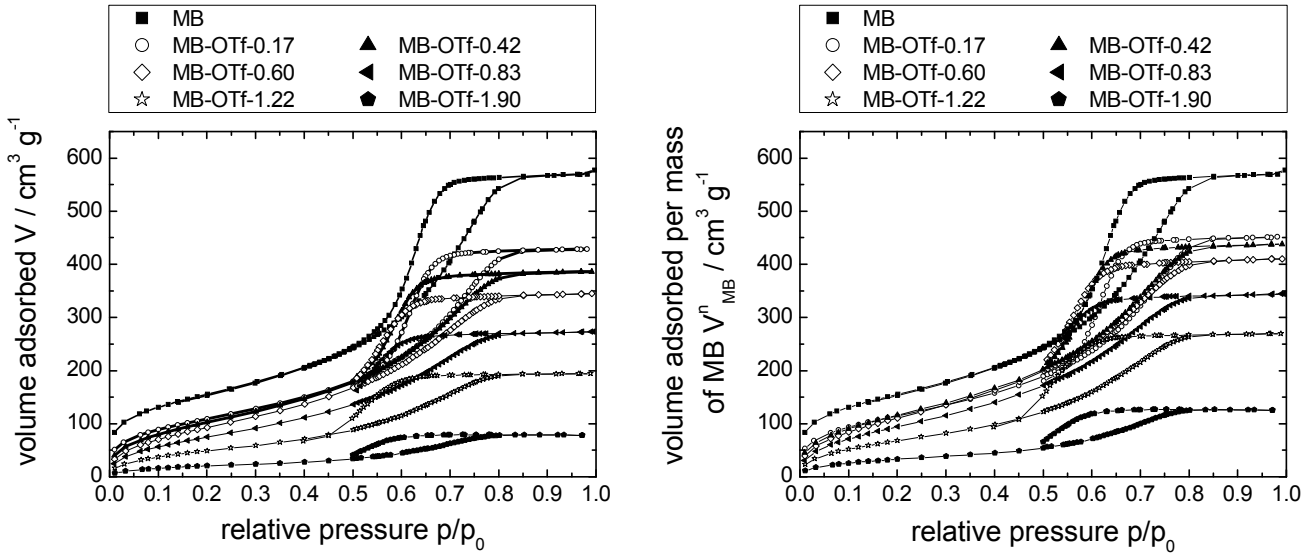

Figure SI 9: N_2-sorption isotherms at 77 K of MB-based materials impregnated with incrementally increasing amounts of [C_6mim][OTf]; as volume absorbed per mass of material (left) and as volume absorbed per mass of support (right).

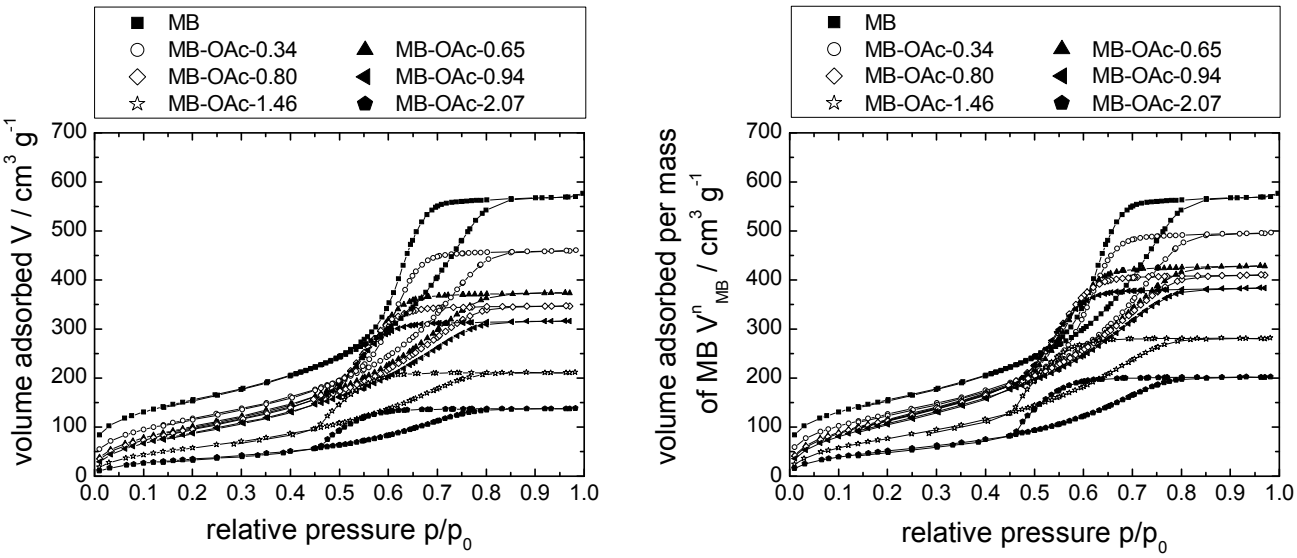

Figure SI 10: N_2-sorption isotherms at 77 K of MB-based materials impregnated with incrementally increasing amounts of [C_6mim][OAc]; as volume absorbed per mass of material (left) and as volume absorbed per mass of support (right).

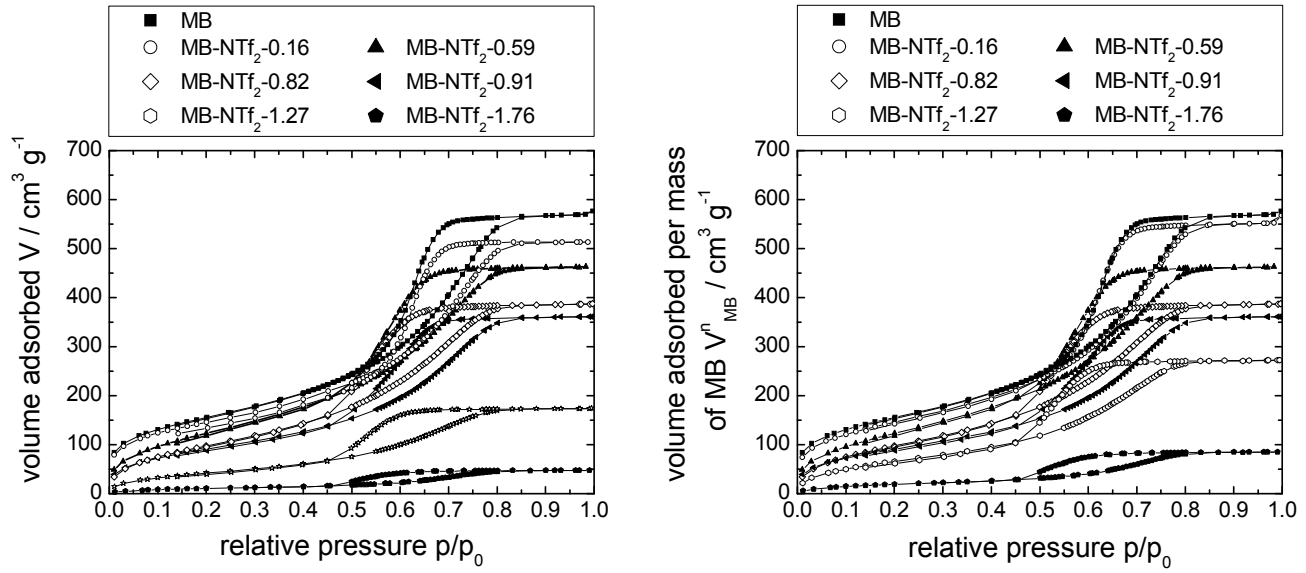

Figure SI 11: N_2-sorption isotherms at 77 K of MB-based materials impregnated with incrementally increasing amounts of [C_6mim][NTf_2]; as volume absorbed per mass of material (left) and as volume absorbed per mass of support (right).

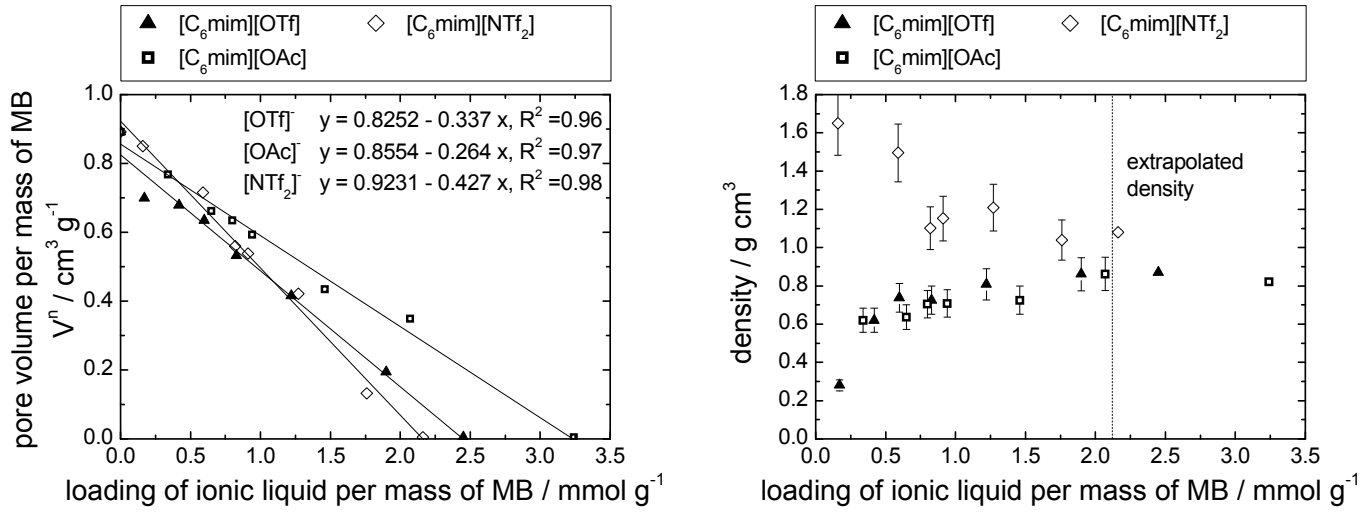

Figure SI 12: Pore volume vs. loading, and density vs. loading of MB modified with incrementally increasing amounts of the ionic liquids investigated.

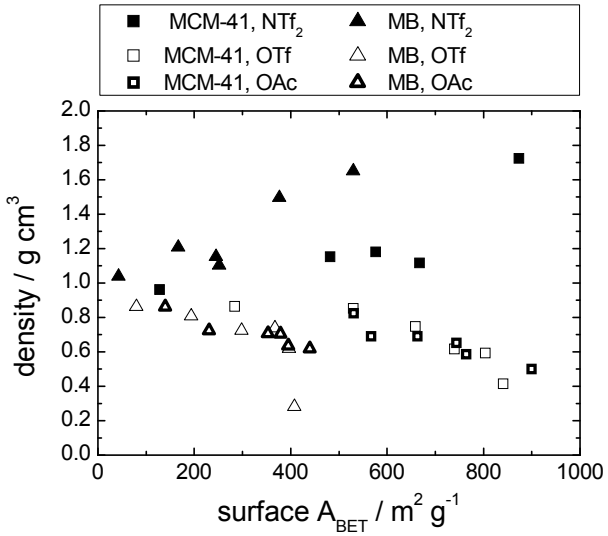

Figure SI 13: Density vs. BET surface of MCM-41 and MB materials.

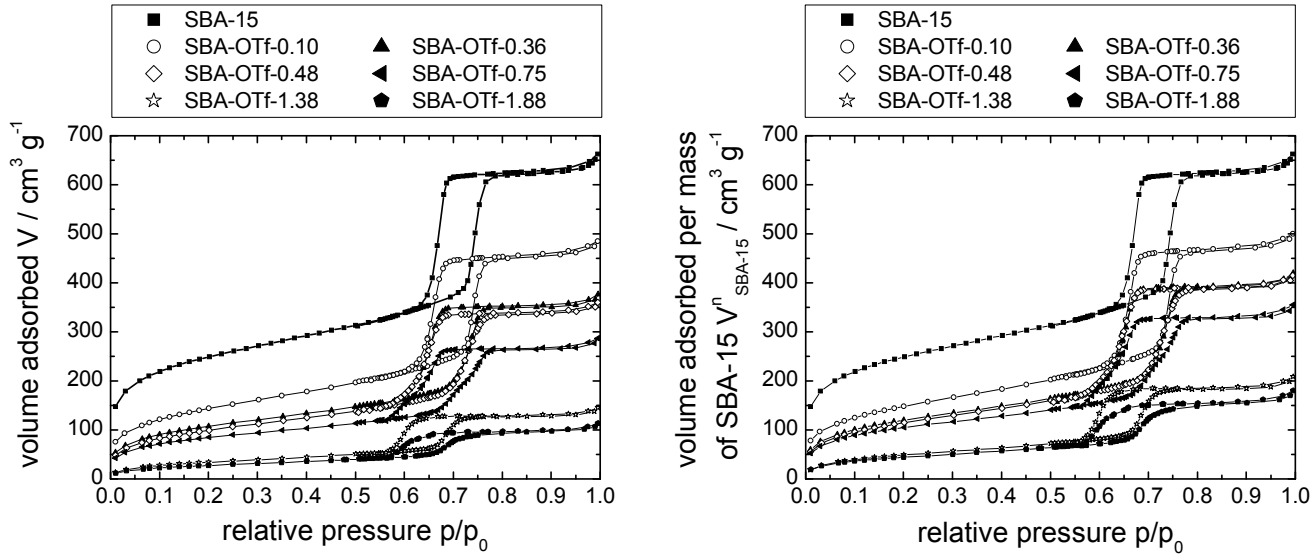

Figure SI 14: N_2-sorption isotherms at 77 K of SBA-based materials impregnated with incrementally increasing amounts of [C_6mim][OTf]; as volume absorbed per mass of material (left) and as volume absorbed per mass of support (right).

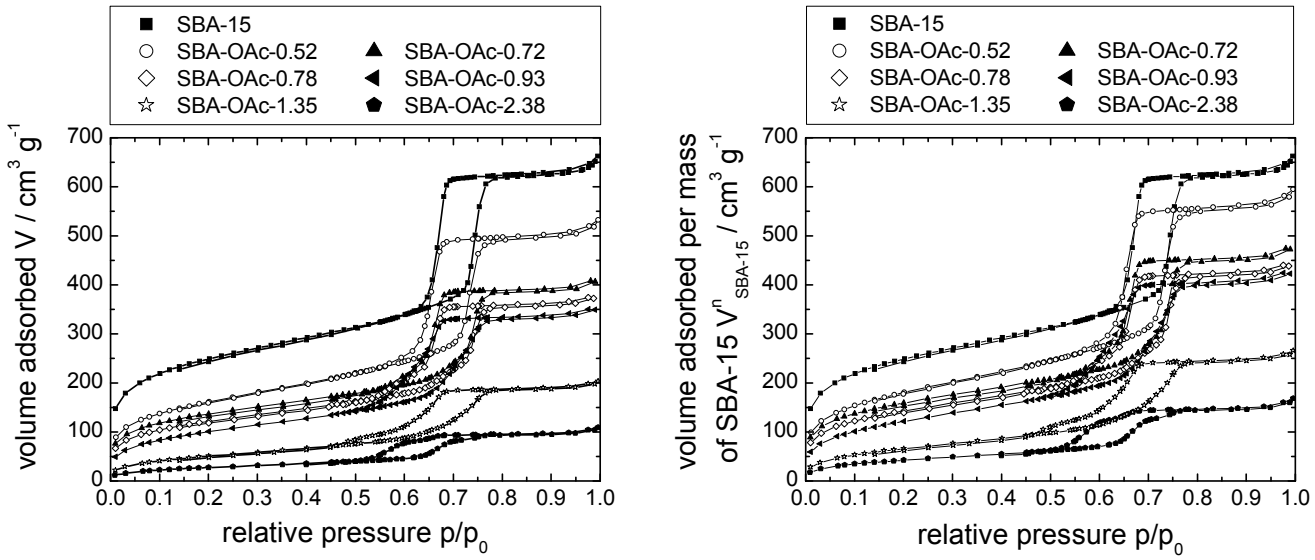

Figure SI 15: N_2-sorption isotherms at 77 K of SBA-based materials impregnated with incrementally increasing amounts of [C_6mim][OAc]; as volume absorbed per mass of material (left) and as volume absorbed per mass of support (right).

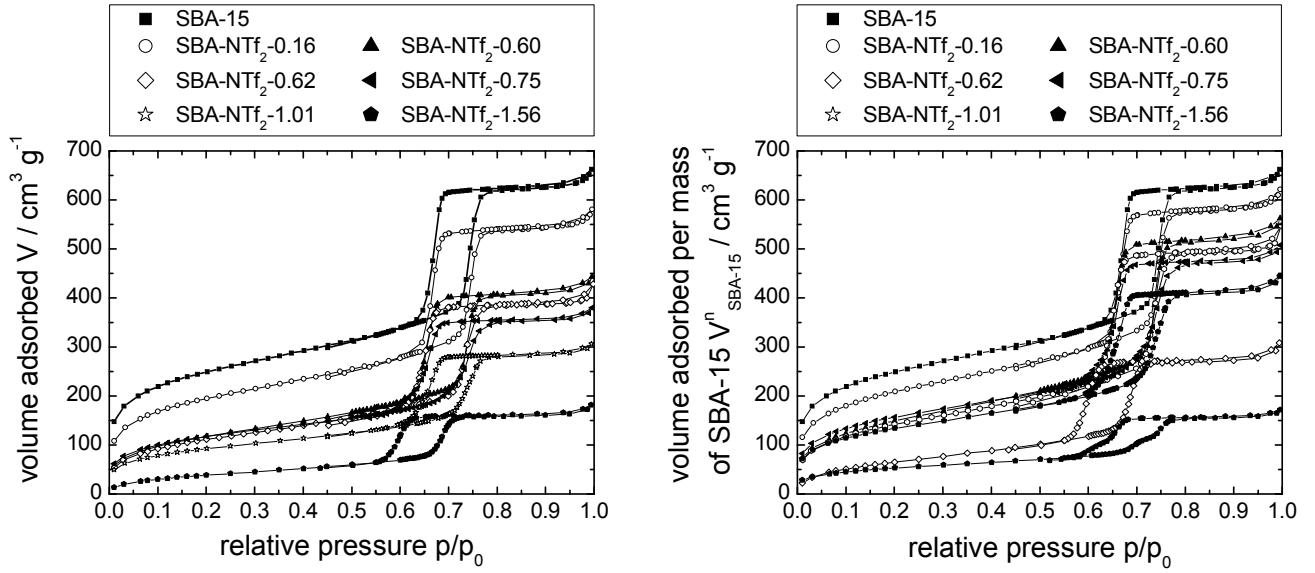

Figure SI 16: N_2-sorption isotherms at 77 K of SBA-based materials impregnated with incrementally increasing amounts of [C_6mim][NTf_2]; as volume absorbed per mass of material (left) and as volume absorbed per mass of support (right).

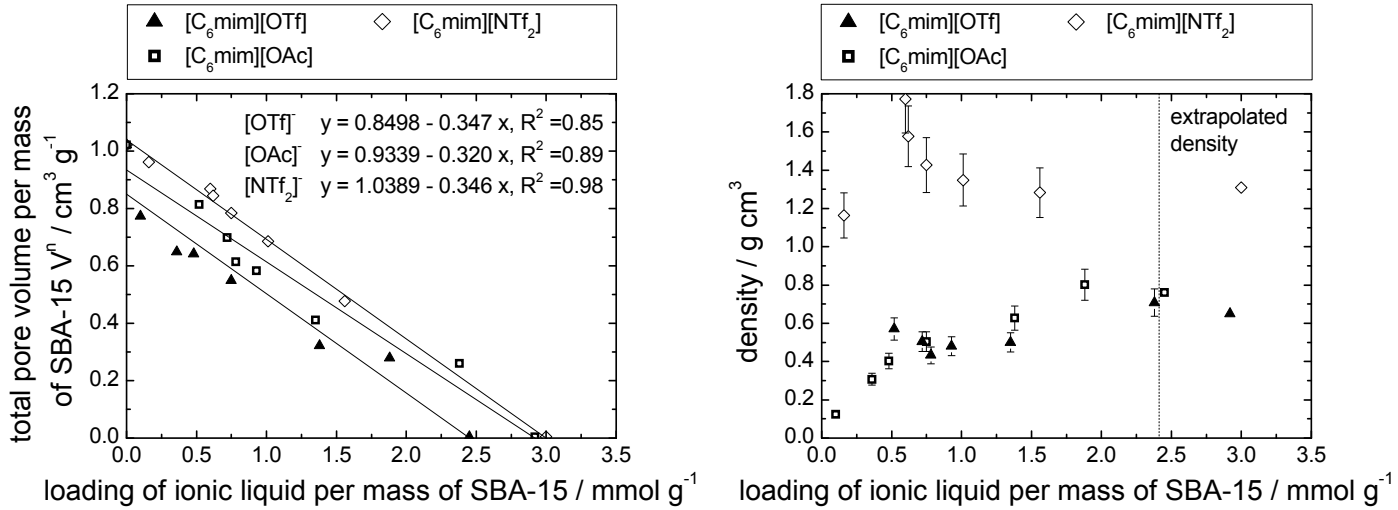

Figure SI 17: Total pore volume vs. loading, and density vs. loading of SBA-15 modified with incrementally increasing amounts of the ionic liquids investigated.

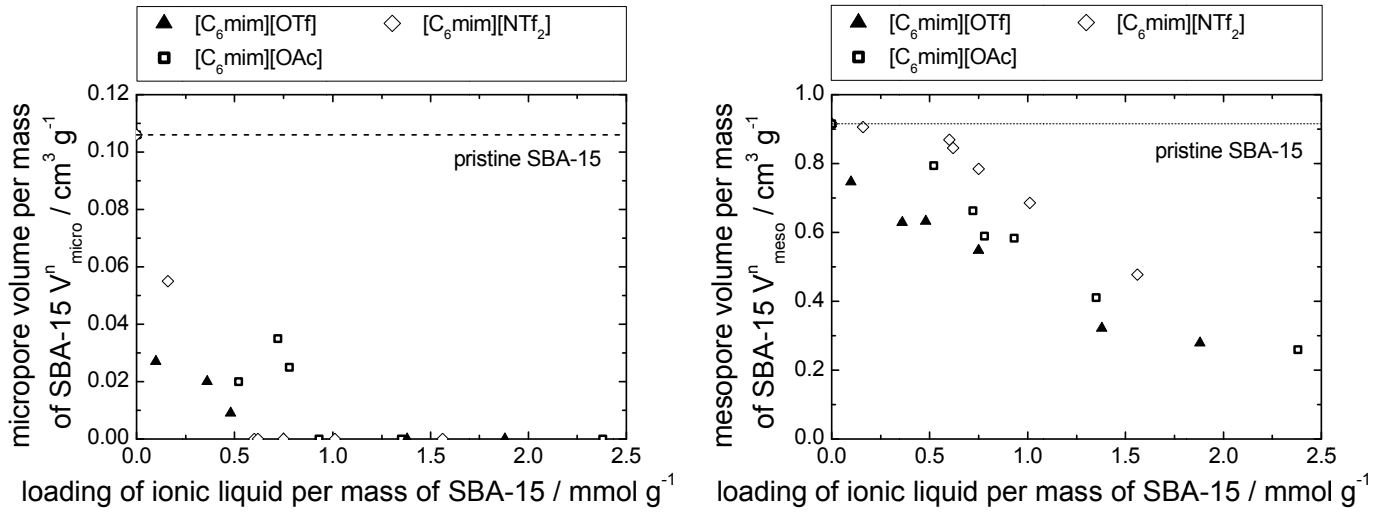

Figure SI 18: Micropore volume vs. loading, and mesopore volume vs. loading of the ionic liquids confined in SBA-15.

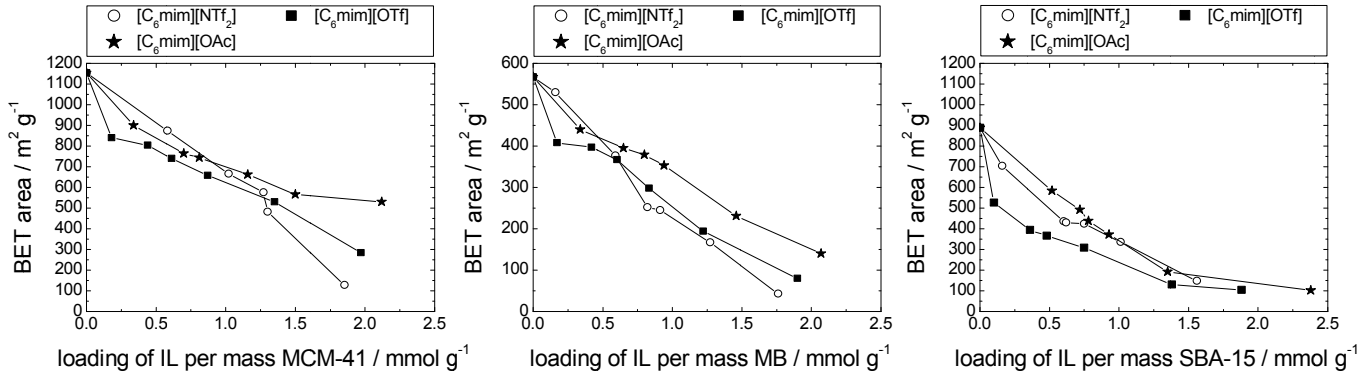

Figure SI 19. BET area vs. loading of $[C_6mim][NTf_2]$, $[C_6mim][OTf]$ and $[C_6mim][OAc]$ on MCM-41 (left), MB (middle) and SBA-15 (right).

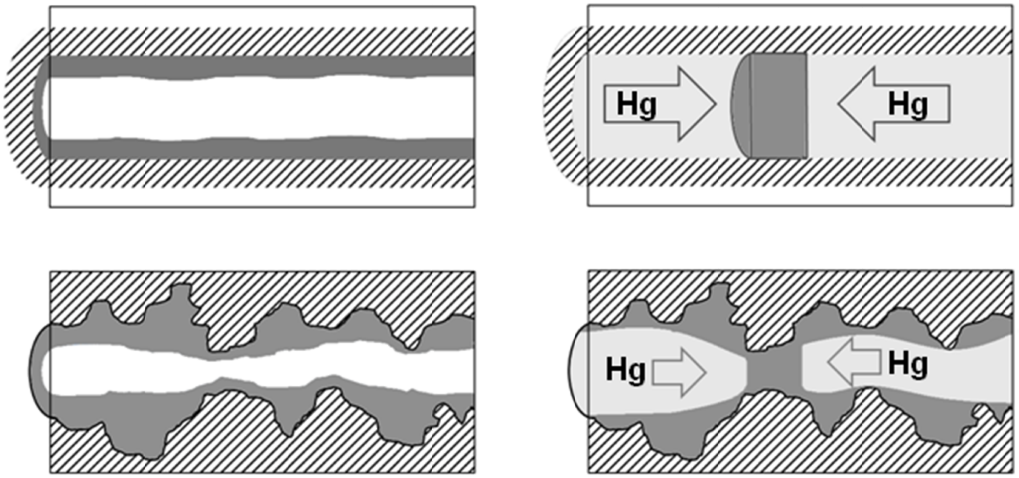

Figure SI 20: Model for the behavior of mercury in SIL-type materials.

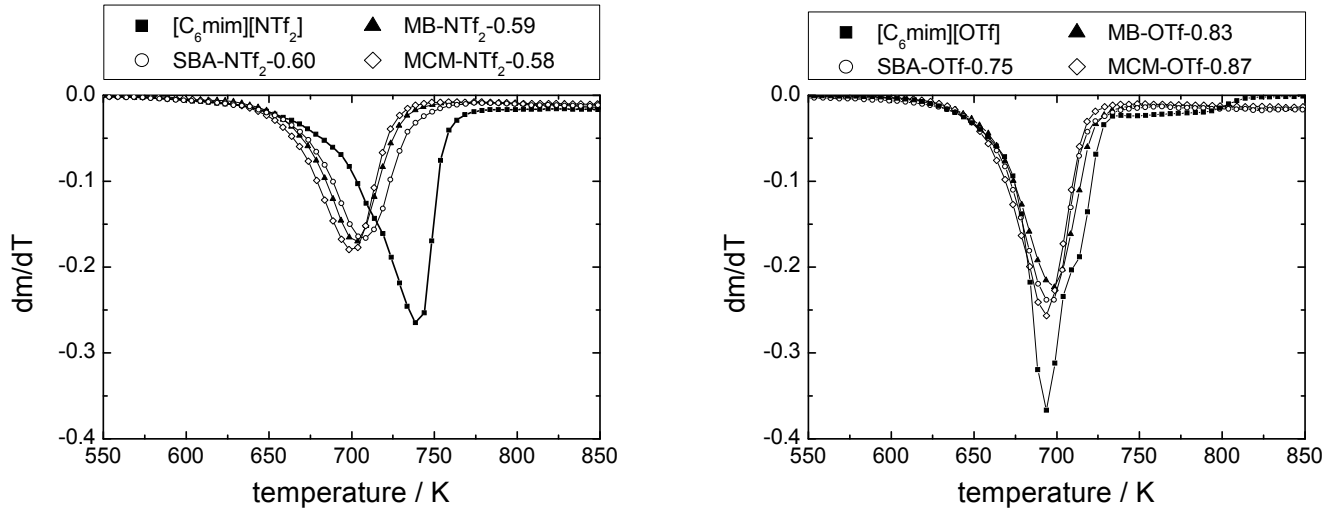

Figure SI 21: DTG signals of [C_6mim][NTf_2], SBA-NTf_2-0.60, MB-NTf_2-0.59 and MCM-NTf_2-0.58 (left) and DTG signals of [C_6mim][OTf], SBA-OTf-0.75, MB-OTf-0.83 and MCM-OTf-0. 87 (right).

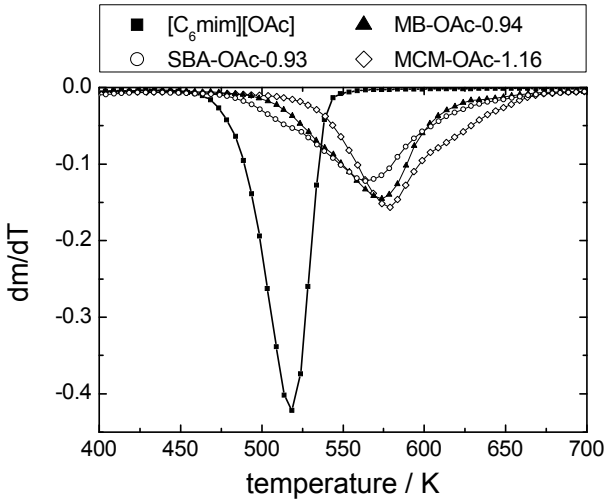

Figure SI 22: DTG signal of [C_6mim][OAc], SBA-OAc-0.93, MB-OAc-0.94 and MCM-OAc-1.16.

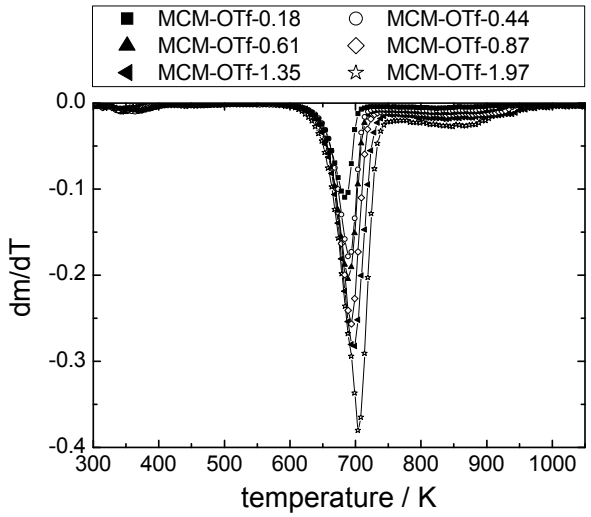

Figure SI 23: DTG of increasing loads of [C_6mim][OTf] on MCM-41.

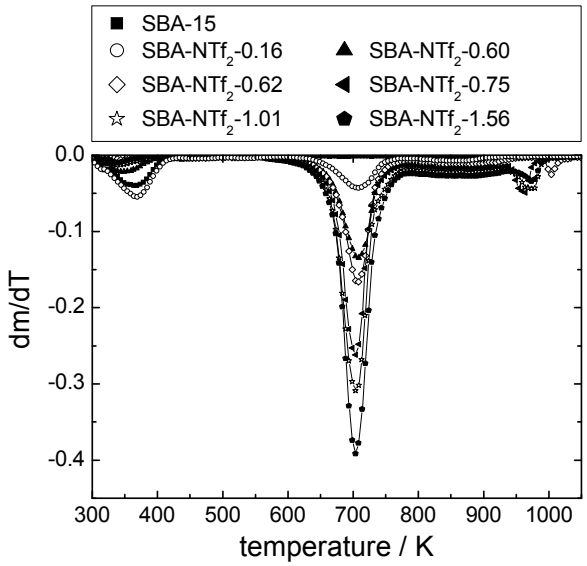

Figure SI 24: DTG of increasing ionic liquid loads of [C_6mim][NTf_2] on SBA-15.

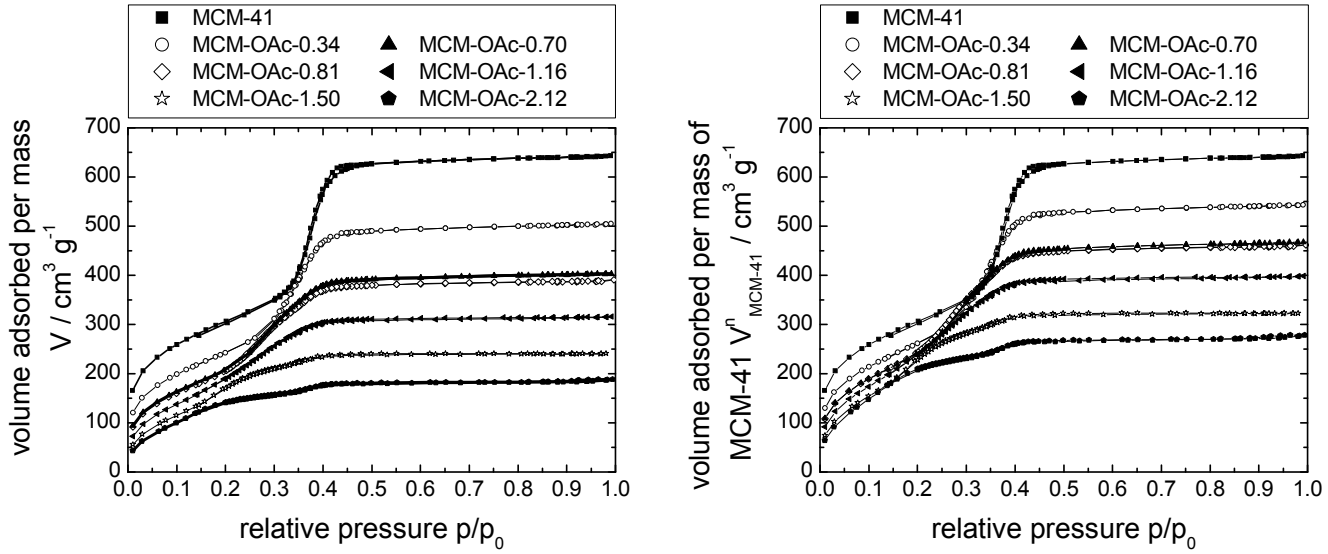

Figure SI 25: Display of all data points measured of Figure 2. N_2-sorption isotherms at 77 K of MCM-41-based materials impregnated with incrementally increasing amounts of [C_6mim][OAc], as volume absorbed per mass of material (left) and as volume absorbed per mass of support (right).

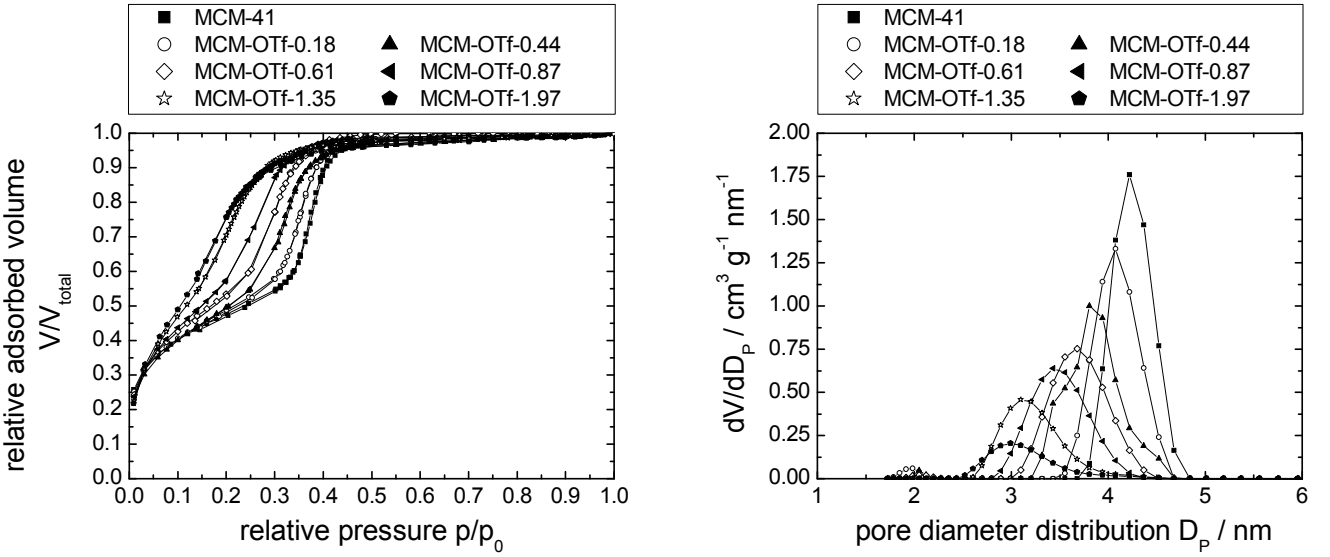

Figure SI 26: Display of all data points measured of Figure 5. N_2-sorption isotherms normalised to the mass of support at 77 K (left) and pore diameter distribution (right) of MCM-41 modified with incrementally increasing amounts of [C_6mim][OTf].

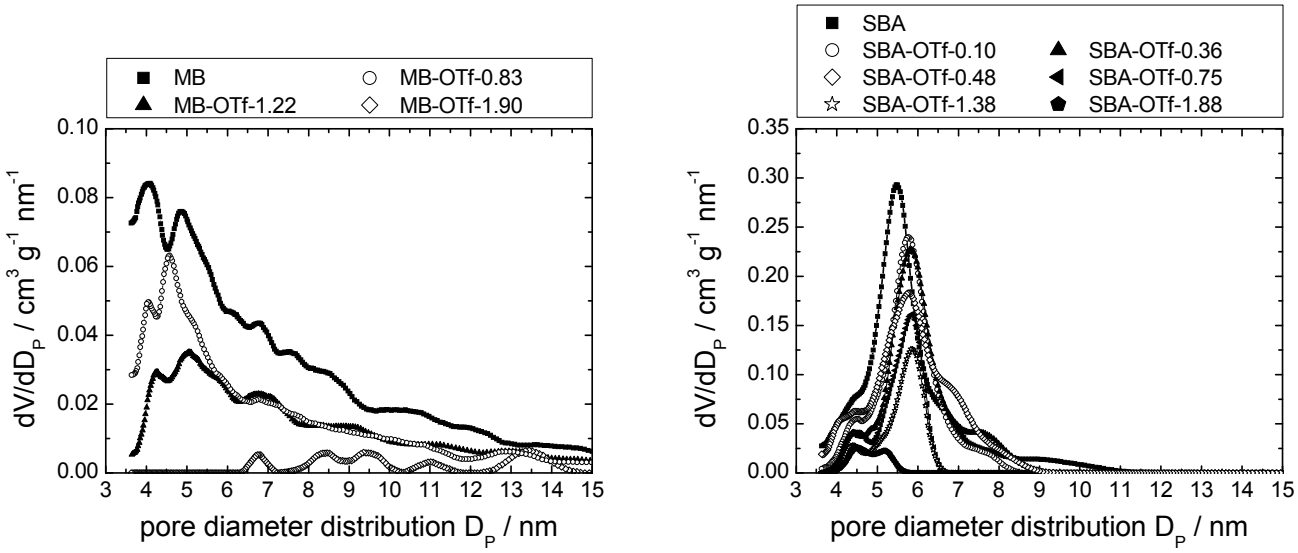

Figure SI 27: Display of all data points measured of Figure 15: Pore diameter distribution profiles determined from Hg-intrusion of MB (left) and SBA-15 (right) with increasing loads of [C_6mim][OTf].

Table SI 1: Characterisation of the pristine MCM-41, and of MCM-41 modified with [C_6mim][OTf], [C_6mim][NTf_2], or [C_6mim][OAc].

Sample	n_{IL} / mmol g^{-1}	V_{meso} / cm^3 g^{-1}	V^n_{meso} / cm^3 g^{-1}	A_{BET} / m^2 g^{-1}	C_{BET}	ρ / g cm^{-3}	α
MCM-41	0.00	1.00	1.00	1155	93	n. a.	0.00
MCM-NTf_2-0.58	0.58	0.67	0.84	874	48	1.7	0.15
MCM-NTf_2-1.02	1.02	0.40	0.59	667	39	1.1	0.41
MCM-NTf_2-1.27	1.27	0.33	0.51	576	13	1.2	0.48
MCM-NTf_2-1.30	1.30	0.31	0.49	482	30	1.2	0.51
MCM-NTf_2-1.85	1.85	0.08	0.14	128	17	1.0	0.86
MCM-OTf-0.18	0.18	0.81	0.86	841	73	0.4	0.18
MCM-OTf-0.44	0.44	0.67	0.76	804	51	0.6	0.33
MCM-OTf-0.61	0.61	0.57	0.68	740	46	0.6	0.43
MCM-OTf-0.87	0.87	0.49	0.63	659	33	0.7	0.51
MCM-OTf-1.35	1.35	0.35	0.49	530	10	0.9	0.65
MCM-OTf-1.97	1.97	0.17	0.27	284	13	0.9	0.83
MCM-OAc-0.34	0.34	0.78	0.84	900	60	0.5	0.22
MCM-OAc-0.70	0.70	0.62	0.72	764	41	0.6	0.37
MCM-OAc-0.81	0.81	0.60	0.71	744	29	0.7	0.39
MCM-OAc-1.16	1.16	0.49	0.62	663	41	0.7	0.51
MCM-OAc-1.50	1.50	0.38	0.50	567	13	0.7	0.62
MCM-OAc-2.12	2.12	0.28	0.41	531	20	0.8	0.72

Note: n_{IL}: mmol ionic liquid per gram support, V_{meso}: mesopore volume, per gram material, V^n_{meso}: mesopore volume, normalised per gram support, A_{BET}: specific surface area, C_{BET}: BET constant, ρ: density of IL at 77 K, α: pore filling degree, n. a. not applicable

Table SI 2: Characterisation of the pristine silica gel (MB), and of MB modified with $[C_6mim][NTf_2]$, $[C_6mim][OTf]$ or $[C_6mim][OAc]$.

Sample	n_{IL} / mmol g^{-1}	V_{meso} / cm^3 g^{-1}	V^n_{meso} / cm^3 g^{-1}	A_{BET} / m^2 g^{-1}	C_{BET}	ρ / g cm^{-3}	α
MB	0.00	0.89	0.89	567	86	n. a.	0.00
MB-NTf_2-0.16	0.16	0.79	0.85	530	97	1.7	0.05
MB-NTf_2-0.59	0.59	0.57	0.72	377	35	1.5	0.20
MB-NTf_2-0.82	0.82	0.41	0.56	252	29	1.1	0.37
MB-NTf_2-0.91	0.91	0.38	0.54	245	43	1.2	0.40
MB-NTf_2-1.27	1.27	0.27	0.42	167	28	1.2	0.53
MB-NTf_2-1.76	1.76	0.07	0.13	43	26	1.0	0.85
MB-OTf-0.17	0.17	0.66	0.70	408	53	0.3	0.22
MB-OTf-0.42	0.42	0.60	0.68	397	34	0.6	0.24
MB-OTf-0.60	0.60	0.53	0.63	367	29	0.7	0.29
MB-OTf-0.83	0.83	0.42	0.53	298	27	0.7	0.40
MB-OTf-1.22	1.22	0.30	0.42	194	28	0.8	0.53
MB-OTf-1.90	1.90	0.12	0.19	80	34	0.9	0.78
MB-OAc-0.34	0.34	0.71	0.77	440	51	0.6	0.14
MB-OAc-0.65	0.65	0.58	0.66	395	32	0.6	0.26
MB-OAc-0.80	0.80	0.54	0.63	379	29	0.7	0.29
MB-OAc-0.94	0.94	0.49	0.59	353	26	0.7	0.34
MB-OAc-1.46	1.46	0.33	0.44	231	25	0.7	0.51
MB-OAc-2.07	2.07	0.24	0.35	140	26	0.9	0.61

Note: n_{IL}: mmol ionic liquid per gram support, V_{meso}: mesopore volume, per gram material, V^n_{meso}: mesopore volume, normalised per gram support, A_{BET}: specific surface area, C_{BET}: BET constant, ρ: density of IL at 77 K, α: pore filling degree, n. a. not applicable

Table SI 3: Characterisation of the pristine SBA-15, and of SBA-15 modified with $[C_6mim][NTf_2]$, $[C_6mim][OTf]$ or $[C_6mim][OAc]$.

Sample	n_{IL} / mmol g^{-1}	V_{micro} / cm^3 g^{-1}	V^n_{micro} / cm^3 g^{-1}	V_{meso} / cm^3 g^{-1}	V^n_{meso} / cm^3 g^{-1}	A_{micro} / m^2 g^{-1}	A_{meso} / m^2 g^{-1}	A_{BET} / m^2 g^{-1}	C_{BET}	ρ / g cm^{-3}	α
SBA-15	0.00	0.11	0.11	0.92	0.92	252	636	888	234	n. a.	0.00
SBA-NTf_2-0.16	0.16	0.05	0.05	0.85	0.91	135	569	704	129	1.2	0.06
SBA-NTf_2-0.60	0.60	0.00	0.00	0.69	0.87	0	436	436	62	1.8	0.15
SBA-NTf_2-0.62	0.62	0.00	0.00	0.66	0.85	0	412	430	65	1.6	0.17
SBA-NTf_2-0.75	0.75	0.00	0.00	0.59	0.78	0	425	425	102	1.4	0.23
SBA-NTf_2-1.01	1.01	0.00	0.00	0.47	0.69	0	336	336	96	1.3	0.33
SBA-NTf_2-1.56	1.56	0.00	0.00	0.28	0.48	0	149	149	34	1.3	0.53
SBA-OTf-0.10	0.10	0.03	0.03	0.72	0.75	30	496	526	83	0.1	0.24
SBA-OTf-0.36	0.36	0.02	0.02	0.57	0.63	0	395	395	78	0.3	0.36
SBA-OTf-0.48	0.48	0.01	0.01	0.55	0.63	0	367	367	70	0.4	0.37
SBA-OTf-0.75	0.75	0.00	0.00	0.44	0.55	0	309	309	86	0.5	0.46
SBA-OTf-1.38	1.38	0.00	0.00	0.22	0.32	0	131	131	42	0.6	0.68
SBA-OTf-1.88	1.88	0.00	0.00	0.18	0.28	0	105	105	51	0.8	0.73
SBA-OAc-0.52	0.52	0.02	0.02	0.71	0.79	56	529	585	104	0.6	0.20
SBA-OAc-0.72	0.72	0.03	0.03	0.57	0.66	78	415	493	137	0.5	0.32
SBA-OAc-0.78	0.78	0.02	0.02	0.50	0.59	58	381	439	120	0.4	0.40
SBA-OAc-0.93	0.93	0.00	0.00	0.48	0.58	0	372	372	66	0.5	0.43
SBA-OAc-1.35	1.35	0.00	0.00	0.32	0.41	0	192	192	45	0.5	0.60
SBA-OAc-2.38	2.38	0.00	0.00	0.17	0.26	0	103	103	53	0.7	0.75

Note: n_{IL}: mmol ionic liquid per gram support, V_{micro}, V_{meso}: micro- resp. mesopore volume, per gram material, V^n_{micro}, V^n_{meso}: micro- resp. mesopore volume, normalised per gram support, A_{micro}, A_{meso}, A_{BET}: micro-, meso and total specific surface area, C_{BET}: BET constant, ρ: density of IL at 77 K, α: pore filling degree, n. a. not applicable

Table SI 4: Characterisation of the pristine MCM-41_NMR, and of MCM-41_NMR modified with $[C_6mim][NTf_2]$.

Sample	n_{IL} / mmol g^{-1}	V_{meso} / cm^3 g^{-1}	V^n_{meso} / cm^3 g^{-1}	A_{BET} / m^2 g^{-1}	C_{BET}	ρ / g cm^{-3}	α
MCM-41_NMR	0.00	1.07	1.07	1136	78	n. a.	0.00
MCM-NTf_2-0.23_NMR	0.23	0.89	0.99	1045	59	1.3	0.16
MCM-NTf_2-0.47_NMR	0.47	0.75	0.91	916	45	1.4	0.30
MCM-NTf_2-0.78_NMR	0.78	0.44	0.59	803	16	0.7	0.59

Note: n_{IL}: mmol ionic liquid per gram support, V_{meso}: mesopore volume, per gram material, V^n_{meso}: mesopore volume, normalised per gram support, A_{BET}: specific surface area, C_{BET}: BET constant, ρ: density of IL at 77 K, α: pore filling degree, n. a. not applicable

Table SI 5: Decomposition temperature of the bulk ionic liquids and of the ionic liquids confined in different silicate-based porous supports (MCM-41, MB and SBA-15).

Sample	temperature / K	sample	temperature / K	sample	temperature / K
[C_6mim][NTf_2]	739	[C_6mim][OTf]	693	[C_6mim][OAc]	519
MCM-NTf_2-0.58	700	MCM-OTf-0.87	693	MCM-OAc-0.94	578
MB-NTf_2-0.59	702	MB-OTf -0.83	697	MB-OAc -1.16	574
SBA-NTf_2-0.60	709	SBA-OTf -0.75	695	SBA-OAc -0.93	564

Table SI 6: Decomposition temperature of [C_6mim][OTf] immobilised on the supports MCM-41, MB and SBA-15 with increasing loads of ionic liquid.

Sample	temperature / K	sample	temperature / K	sample	temperature / K
MCM-OTf-0.18	684	MB-OTf-0.17	693	SBA-OTf-0.10	698
MCM-OTf-0.44	689	MB-OTf-0.42	695	SBA-OTf-0.36	698
MCM-OTf-0.61	689	MB-OTf-0.60	697	SBA-OTf-0.48	693
MCM-OTf-0.87	693	MB-OTf-0.83	697	SBA-OTf-0.75	695
MCM-OTf-1.35	695	MB-OTf-1.22	696	SBA-OTf-1.38	693
MCM-OTf-1.97	704	MB-OTf-1.90	707	SBA-OTf-1.88	690

Table SI 7: Decomposition temperature of [C_6mim][NTf_2] immobilised on the supports MCM-41 and MB with increasing loads of ionic liquid.

Sample	temperature / K	sample	temperature / K
MB-NTf_2-0.16	695	SBA-NTf_2-0.16	708
MB-NTf_2-0.59	702	SBA-NTf_2-0.60	709
MB-NTf_2-0.82	703	SBA-NTf_2-0.62	706
MB-NTf_2-0.91	704	SBA-NTf_2-0.75	704
MB-NTf_2-1.27	707	SBA-NTf_2-1.01	704
		SBA-NTf_2-1.56	704